Lithium Chloride Exerts Anti-Inflammatory and Neuroprotective Effects by Inhibiting Microglial Activation in LPS-Induced Retinal Injury

Nandan Wu, Qian Luo, Yuke Huang, Linxi Wan, Xiangtao Hou, Zihua Jiang, Yan Li, Jin Qiu, Pei Chen, Keming Yu, Jing Zhuang, and Ying Yang

State Key Laboratory of Ophthalmology, Zhongshan Ophthalmic Center, Sun Yat-Sen University, Guangdong Provincial Key Laboratory of Ophthalmology and Visual Science, Guangzhou, People's Replubic of China

Correspondence: Jing Zhuang, State Key Laboratory of Ophthalmology, Zhongshan Ophthalmic Center, Sun Yat-Sen University, Guangdong Provincial Key Laboratory of Ophthalmology and Visual Science, Guangzhou 510060, P. R. China; zhuangj@mail.sysu.edu.cn.
Ying Yang, State Key Laboratory of Ophthalmology, Zhongshan Ophthalmic Center, Sun Yat-Sen University, Guangdong Provincial Key Laboratory of Ophthalmology and Visual Science, Guangzhou 510060, P. R. China; yangy568@mail.sysu.edu.cn.

PURPOSE. To explore the anti-inflammatory and neuroprotective effects of lithium chloride (LiCl) in LPS-induced retinal injury.

METHODS. In vitro, primary retinal microglia were pretreated with LiCl and stimulated with lipopolysaccharide (LPS). Pro-inflammatory cytokine production, microglial morphological changes, and inflammation-associated signaling pathways were measured by real-time PCR (RT-PCR), western blotting, and immunofluorescence. Primary retinal neurons were cultured with microglial-derived conditioned medium in the absence or presence of LiCl. Neurotoxicity was evaluated by Cell Counting Kit-8 (CCK-8), terminal deoxynucleotidyl transferase-mediated dUTP nick end labeling (TUNEL) assay, and γ-H2AX detection. In vivo, an endotoxin-induced uveitis mice model was established, and each animal was given intraperitoneal injection of LiCl or vehicle. The retinal inflammatory response was measured by hematoxylin and eosin and fluorescent staining, RT-PCR, western blotting, and TUNEL assay. Retinal thickness and function were evaluated by spectral-domain optical coherence tomography and electroretinography.

RESULTS. In vitro, LiCl exerted no obvious toxic effects on microglia and significantly decreased proinflammatory factor (inducible nitric oxide synthase, tumor necrosis factor α, interleukin 6) production, inhibited microglial activation in morphology, and suppressed nuclear factor kappa B (NF-κB), Akt, and phosphatidylinositol 3-kinase (PI3K) phosphorylation. Moreover, LiCl promoted retinal neuron survival and reduced cell apoptosis and the expression of γ-H2AX. In vivo, LiCl reduced inflammatory infiltrating cells in the vitreous cavity and decreased proinflammatory cytokine expression in retinas. LiCl suppressed LPS-induced microglial activation, proliferation, and migration. Additionally, LiCl reduced LPS-induced apoptosis of ganglion cells and retinal edema and rescued retinal functional damage.

CONCLUSIONS. This study demonstrates that LiCl exerts anti-inflammatory and neuroprotective effects by inhibiting microglial activation via the PI3K/Akt/NF-κB pathway in LPS-induced retinal injury. LiCl provides a novel and promising option to treat retinal inflammatory diseases.

Keywords: lithium chloride (LiCl), microglia, retinal inflammation, neuroprotection

Retinal inflammation is a common pathophysiological process in numerous retinal diseases, including age-related macular degeneration, retinitis pigmentosa, diabetic retinopathy, and uveitis, and it contributes to visual impairment and even blindness.[1] Recently, massive evidence has suggested that microglial activation plays a key role in initiating and maintaining retinal inflammation.

Microglia are the essential resident immune cells in the brain and retina and constitute the first line of defense against stimuli.[2–4] Under physiological conditions, microglia maintain a characteristic ramified morphology with high motility, helping phagocytose dead cells and maintaining retinal homeostasis and normal function of protein aggregates, cellular debris, and invading pathogens. However, pathologically activated microglia can constantly secrete multiple proinflammatory mediators, such as tumor necrosis factor α (TNF-α), interleukin-6 (IL-6), and nitric oxide, which leads to the occurrence of neuroinflammation. In addition, these proinflammatory mediators also further activate microglia in a vicious cycle that aggravates the neuronal dysfunction and neurodegeneration.[5] Therefore, the inhibition of microglial overactivation has been identified as a novel therapeutic strategy to manage retinal inflammatory diseases.

Lithium chloride (LiCl) is an effective mood stabilizer that has been used to treat bipolar disorder (BD) in the clinic for more than 50 years. Numerous studies on the mechanism have reported the therapeutic efficacy of LiCl and

suggest that its anti-inflammatory effect may play an important role.[6,7] More importantly, with regard to some brain diseases, much evidence from both in vitro and in vivo studies has demonstrated that LiCl acts as a powerful anti-inflammatory agent by inhibiting microglial activation. As an example, pretreatment with LiCl could inhibit lipopolysaccharide (LPS)-induced primary brain microglial activation and proinflammatory cytokine production via the phosphatidylinositol 3-kinase (PI3K)/Akt/forkhead box protein O1 (FoxO1) signaling pathway.[8] In chronic, mild stress-exposed rats, LiCl treatment suppressed microglial activation in the hippocampus and alleviated neuroinflammation by regulating Wnt/β-catenin signaling.[9] However, it is not clear whether LiCl regulates retinal inflammatory responses by inhibiting microglial activation.

The ideal drug for treating retinal inflammatory diseases should possess powerful anti-inflammatory effects and exert protective activity on neurons. Interestingly, various studies have demonstrated the potential neuroprotective effect of lithium against various insults, such as cerebral ischemia–reperfusion injury, cold-induced traumatic brain injury, and other neurodegenerative conditions.[10–12] Moreover, in our previous study, LiCl protected retinal neurocytes from ischemia-induced damage by enhancing DNA nonhomologous end-joining repair.[13] However, whether LiCl protects retinal neurons against inflammation-mediated toxicity is still unclear.

To answer this question, we cultured primary retinal microglia and neurons in vitro and established an endotoxin-induced uveitis (EIU) model to investigate whether LiCl treatment can alleviate retinal inflammation by inhibiting microglial activation, protect retinal neurons against inflammation-induced damage, and rescue visual function. Our study suggests that LiCl may be an ideal drug to treat retinal inflammatory diseases.

MATERIALS AND METHODS

Animals

Adult and newborn (P1–P3) C57BL/6J mice were purchased from the Laboratory Animal Center at Sun Yat-sen University. All animal experiments were handled following the ARVO Statement on the Use of Animals in Ophthalmic and Vision Research and were approved by the Institutional Animal Ethical Committee of Zhongshan Ophthalmic Center, Sun Yat-sen University (permit number SYXK [YUE] 2020-155).

Primary Cell Culture

Newborn (P1–P3) C57BL/6J mice were used to prepare the primary cell culture. For primary retinal microglia culture, the protocol followed the previous study with some modifications.[14] Briefly, mice retinas were isolated and treated with 0.125% trypsin–EDTA to obtain single-cell suspensions. Next, the cells were seeded in T75 flasks and cultured in Dulbecco's Modified Eagle Medium/Nutrient Mixture F-12 (DMEM/F-12) medium containing 20% fetal bovine serum and 1% penicillin streptomycin (PS). Three weeks after the implantation, retinal microglia were isolated from the mixed glial cells by shaking at 200 rpm for 1 hour and were further purified by differential adhesion method for 30 minutes. For primary retinal neuron culture, single-cell suspensions were prepared in the same way as the microglia culture. The cells were then plated in dishes with Neurobasal-A Medium

(Thermo Fisher Scientific, Waltham, MA, USA) containing 2-mM glutamine, 1% PS, and 2% B-27 supplements. The retinal microglia and neurons were identified by staining with ionized calcium binding adaptor molecule 1 (IBA1) and microtubule-associated protein-2 (MAP2) antibodies, respectively. All cells were cultured in a humidified atmosphere of 5% carbon dioxide at 37°C. The cell culture media and reagents were purchased from Thermo Fisher Scientific.

Primary Retinal Microglia Treatment

Primary retinal microglia were treated with different concentrations of LiCl (0, 0.5, 1, and 2 mM) for 12 hours or 24 hours. Microglia were divided into three groups: (1) control, (2) LPS treatment, and (3) LPS + LiCl treatment. The cells were pretreated with PBS or LiCl (1 mM) for 30 minutes and then activated by 20 ng/mL LPS (Sigma-Aldrich, St. Louis, MO, USA) for 12 hours or 24 hours. For the nuclear factor kappa B (NF-κB) inhibitor study, microglia were pretreated with BAY-11-7082 (1 mM; Cayman Chemical, Ann Arbor, MI, USA) for 2 hours, followed by activation with 20 ng/mL LPS for 12 hours.

Microglial-Derived Conditioned Medium Preparation and Primary Retinal Neuron Treatment

The primary retinal microglia (5×10^5 cells/mL) were seeded in 10-cm dishes and treated with LPS (0.5 µg/mL) or PBS for 30 minutes. The cells were then washed twice with PBS and cultured in fresh complete medium. After another 24-hour culture, the microglial-derived conditioned medium (MCM) and normal microglial-derived media were collected and then centrifuged at 150g for 5 minutes prior to displacing the cell debris. Primary retinal neurons were divided into three groups: (1) control, (2) MCM treatment, and (3) MCM + LiCl treatment. The cells in groups 2 and 3 were pretreated with PBS or LiCl (1 mM) for 30 minutes, and the media were then replaced by normal microglial-derived media in group 1, MCM in group 2, and MCM + LiCl (1 mM) in group 3. The cells were harvested after another 48-hour culture for further analysis.

Cell Viability Assay

Cell viability was tested using a Cell Counting Kit-8 (CCK-8; Biosharp, Hefei City, China). CCK-8 reagent was added to each well, followed by incubation for 2 hours, and the absorbance (optical density) was determined at 450 nm using a fluorescence plate reader (BioTek Power Wave XS; Agilent, Santa Clara, CA, USA). Relative cell viability was determined by the optical density ratio of treated cells over the control.

Reverse Transcription–Quantitative Polymerase Chain Reaction

Total RNA from microglia or retinas were extracted using TRIzol reagent (Thermo Fisher Scientific) according to the manufacturer's protocol, followed by treatment with DNAse I to remove DNA contaminants. The RNA was then reverse transcribed into cDNA by using a SYBR PrimeScript RT-PCR Kit (Takara Biomedical Technology, Beijing, China). The cDNA was amplified by PCR using a LightCycler 480 II

TABLE 1. Primer Sequences for Quantitative Real-Time PCR

Gene		Primer Sequence (5′∼3′)
iNOS	Forward	ACATCGACCCGTCCACAGTAT
	Reverse	CAGAGGGGTAGGCTTGTCTC
IL-6	Forward	CTTCACAAGTCGGAGGCTTA
	Reverse	TTCTGCAAGTGCATCATCGT
TNF-α	Forward	CCACCACGCTCTTCTGTCTA
	Reverse	AGGGTCTGGGCCATAGAACT
β-Actin	Forward	AGGTCATCACTATTGGCAACG
	Reverse	ACGGATGTCAACGTCACACTT

Sequence Detection System (Roche, Basel, Switzerland). The target genes were detected with primer sequences listed in Table 1. The quantification of target genes was calculated using the $2^{-\Delta\Delta CT}$ method.

Protein Extraction and Western Blot

Treated cells and retinas were collected for whole protein extraction by using radioimmunoprecipitation assay lysis buffer containing protease inhibitor (Beijing Biotech, Beijing, China) according to the manufacturer's protocol. Protein concentration was quantified using the BCA Protein Assay Kit (Solarbio Science & Technology, Beijing, China). Equal amounts of protein (30 μg) were separated on an 8% to 12.5% SDS-PAGE gel and transferred to a polyvinylidene fluoride membrane. The membranes were blocked with 5% BSA and incubated with primary antibodies at 4°C overnight (Table 2). The membranes were further incubated with horseradish peroxidase–conjugated secondary antibody (Cell Signaling Technology, Danvers, MA, USA) and subsequently visualized using an enhanced chemiluminescence system. Bio-Rad Image Lab 5.1 software (Bio-Rad, Hercules, CA, USA) was used for quantification. The uncropped gel images are presented in Supplemental Figure S1.

Immunofluorescence

Treated cells and retinal cryosections were fixed with 4% paraformaldehyde (PFA) for 20 minutes, incubated with 0.1% Triton X-100 for 10 minutes, and then blocked with 10% normal goat serum for 30 minutes. Subsequently, samples were incubated at 4°C overnight with the primary antibodies listed in Table 2. Alexa Fluor 488 anti-Rabbit IgG and Alexa Fluor 555 anti-Mouse IgG (Cell Signaling Technology) were used as secondary antibodies, and nuclei were stained with 4′,6-diamidino-2-phenylindole (DAPI). Images were captured using a confocal microscope (LSM 980; Carl Zeiss Microscopy, Jena, Germany). The immunofluorescence intensity was quantified using Image J software (National Institutes of Health, Bethesda, MD, USA).

Enzyme-Linked Immunosorbent Assay

Cell supernatants were collected to analyze the level of proinflammatory cytokines (IL-6 and TNF-α) by using enzyme-linked immunosorbent assay (ELISA) kits (Elabscience Biotechnology, Wuhan, China) following the manufacturer's instructions. The optical density value was measured at 450 nm by the microplate reader.

EIU Mice Model and Treatment

According to the previous study, the EIU model was induced by intravitreal injection of LPS for the retinal inflammation study.[14–16] Adult female C57BL/6J mice were randomly divided into three groups: (1) control, (2) LPS treatment, and (3) LPS + LiCl treatment. The right eyes of mice were intravitreally injected with 1 μL PBS (group 1) or 1 μL of 200 μg/mL LPS (groups 2 and 3). The mice in group 3 received intraperitoneal injections of LiCl (40 mg/kg) at three time points—1 day before, 3 hours before, and 3 hours after LPS intravitreal injection—and the mice in groups 1 and 2 received the

TABLE 2. Antibodies for Western Blot and Immunofluorescence

	Antibodies	Cat. No.	Manufacturer
Western blot	Anti-NF-κB	8242	Cell Signaling Technology
	Anti-p-NF-κB	3033	Cell Signaling Technology
	Anti-IκBα	4814	Cell Signaling Technology
	Anti-p-IκBα	2859	Cell Signaling Technology
	Anti-PI3K	4257	Cell Signaling Technology
	Anti-p-PI3K	4228	Cell Signaling Technology
	Anti-Akt	9272	Cell Signaling Technology
	Anti-p-Akt	4060	Cell Signaling Technology
	Anti-γ-H2AX	2577	Cell Signaling Technology
	Anti-Bcl-2	4223	Cell Signaling Technology
	Anti-BAX	5023	Cell Signaling Technology
	Anti-caspase 3	9665	Cell Signaling Technology
	Anti-tubulin	2148	Cell Signaling Technology
	Anti-iNOS	GTX-130246	GeneTex
	Anti-TNF-α	60291-1-lg	Proteintech
	Anti-IL-6	GB11117	Servicebio Biological
Immunofluorescence	Anti-NF-κB	8242	Cell Signaling Technology
	Anti-IBA1	ab178847	Abcam
	Anti-MAP2	BM1243	Boster Bio
	Anti-γ-H2AX	2577	Cell Signaling Technology
	Anti-IBA1	ab283319	Abcam
	Anti-Ki67	MA5-14520	Invitrogen
	Anti-RBPMS	GTX-118619	GeneTex

same amount of PBS. Further experiments were performed 24 hours after the LPS stimulation.

Histopathological Analysis

The mice eyeballs ($n = 5$ in each group) were fixed in PFA for 24 hours, dehydrated with gradient ethanol (65%, 75%, 85%, 95%, and 100%), and then embedded in paraffin. The blocks were cut through the optic disk at 5μm thickness, deparaffinized, and stained with a hematoxylin and eosin (H&E) kit (DH0006-2; Leagene Biotech, Beijing, China) according to the manufacturer's instructions. The sections were photographed using a Leica DM4000 microscope (Leica Microsystems, Wetzlar, Germany). Three images in each eye were randomly captured in a field centered on the optic disc. The counting of inflammatory cells was performed by two experienced researchers using Image J software, and the averages of the determinations by each researcher were documented.

Retinal Flat-Mount Preparation and Immunofluorescence Assay

Extracted eyeballs ($n = 4$ in each group) were fixed in 4% PFA for 30 minutes, and the entire retinas were then carefully dissected from the eyecup and blocked in PBS containing 5% BSA and 0.5% Triton X-100 at room temperature (RT) for 2 hours. Next, the retinas were single stained with primary antibody against IBA1 or double stained with IBA1 and Ki67 overnight at 4°C, followed by incubation with Alexa Fluor 488 anti-Rabbit IgG and Alexa Fluor 555 anti-Mouse IgG antibody at RT for 2 hours. Subsequently, retinas were flattened onto glass slides by cutting four radial incisions, and they were photographed using a confocal microscope. Four images per retina at the mid-periphery were captured. For morphological analysis of the microglia, the images were converted into skeletonized images, and the branch number and average branch length of microglia were quantified using Image J software with the AnalyzeSkeleton (2D/3D) plugin. To evaluate the microglia proliferative activity, co-labeled Ki67$^+$/IBA1$^+$ cells were counted using Image J software.

Terminal Deoxynucleotidyl Transferase dUTP Nick End Labeling Assay

For primary retinal neurons, apoptotic assay was performed using a terminal deoxynucleotidyl transferase dUTP nick end labeling (TUNEL) kit (Roche) according to the manufacturer's instructions. In brief, the cells were incubated with TUNEL reaction mixture for 1 hour at 37°C in the dark, and the nuclei were stained with DAPI for 5 minutes. The assay was performed three times. Each time, five images in each group were randomly captured using a confocal microscope for quantization. For retinas ($n = 3$ in each group), the retinal cryosections were stained with RNA-binding protein with multiple splicing (RBPMS; a retinal ganglion cell [RGC] marker) and TUNEL double staining. After TUNEL staining, the sections were stained by immunofluorescence using the above method with anti-RBPMS antibody (GeneTex, Irvine, CA, USA). Alexa Fluor 555 anti-Rabbit IgG was used as a secondary antibody, and nuclei were stained with DAPI. Five images were randomly captured in each retina using a confocal microscope.

Spectral-Domain Optical Coherence Tomography

Total retinal thickness was measured by optical coherence tomography (OCT; (SPECTRALIS, Heidelberg, Germany). Mice ($n = 5$) were anesthetized by intraperitoneal injection with ketamine (100 mg/kg) and xylazine (10 mg/kg), and pupils were dilated with 2.5% phenylephrine and 0.5% tropicamide before image acquisition. The mean total retinal thickness was calculated within a circle of 3.45-mm radius from the optic nerve head using Heidelberg Eye Explorer software.

Electroretinogram Recordings

After overnight dark adaptation, electroretinogram (ERG) recordings of mice ($n = 5$ in each group) were performed using a RETI-port/scan 21 system (Roland Consult, Brandenburg an der Havel, Germany). The mice were anesthetized with ketamine (100 mg/kg) and xylazine (10 mg/kg). After pupil dilation and ocular surface anesthesia, a gold-plated wire loop electrode was placed at the corneal surface and stainless steel needles were inserted into the skin near the eye and into the tail to serve as the active electrode, reference electrode, and ground electrode, respectively. Subsequently, eyes were stimulated with 0.3 and 3.0 cd·s/m^2 intensity levels of a light flash under dark-adapted conditions and with 3.0 cd·s/m^2 light intensity under light-adapted conditions; the a-wave and b-wave amplitudes were recorded and analyzed.

Statistical Analysis

Data are presented as mean $\pm$ SD, and comparisons of multiple groups were analyzed using one-way analysis of variance (ANOVA) followed by Tukey's or Dunnett's T3 post hoc test using SPSS Statistics 21.0 (IBM, Chicago, IL, USA). A value of $P < 0.05$ was considered statistically significant. All experiments were repeated at least three times.

RESULTS

LiCl Inhibits Inflammatory Factor Production and Retinal Microglial Activation In Vitro

First, the CCK-8 assay was performed to evaluate the toxic effects of LiCl on primary retinal microglia. The results showed that LiCl exerted no obvious toxic effects on microglia at any tested dose (0, 0.5, 1, or 2 mM) (Fig. 1A). Then, we pretreated microglia with LiCl at different doses (0, 0.5, 1, or 2 mM) for 30 minutes, followed by activation with 20 ng/mL LPS. The application of LPS significantly increased inducible nitric oxide synthase (iNOS) mRNA expression, but LiCl inhibited this effect in a dose-dependent manner (Fig. 1B). Thus, based on our previous study,[13] 1 mM of lithium was selected for the subsequent experiments. Similarly, altered iNOS protein expression was consistent with the change in mRNA levels (Figs. 1C, 1D). In addition, LiCl notably reduced LPS-induced TNF-α and IL-6 mRNA expression and protein secretion upregulation via real-time PCR (RT-PCR) and ELISA detection (Figs. 1E, 1F). Subsequently, IBA1 immunostaining was used to observe microglial morphological changes. As shown in Figure 1G, the control retinal microglia were thin cell bodies with branched extensions. When stimulated with LPS, the cells were activated and became rounder and more ameboid in
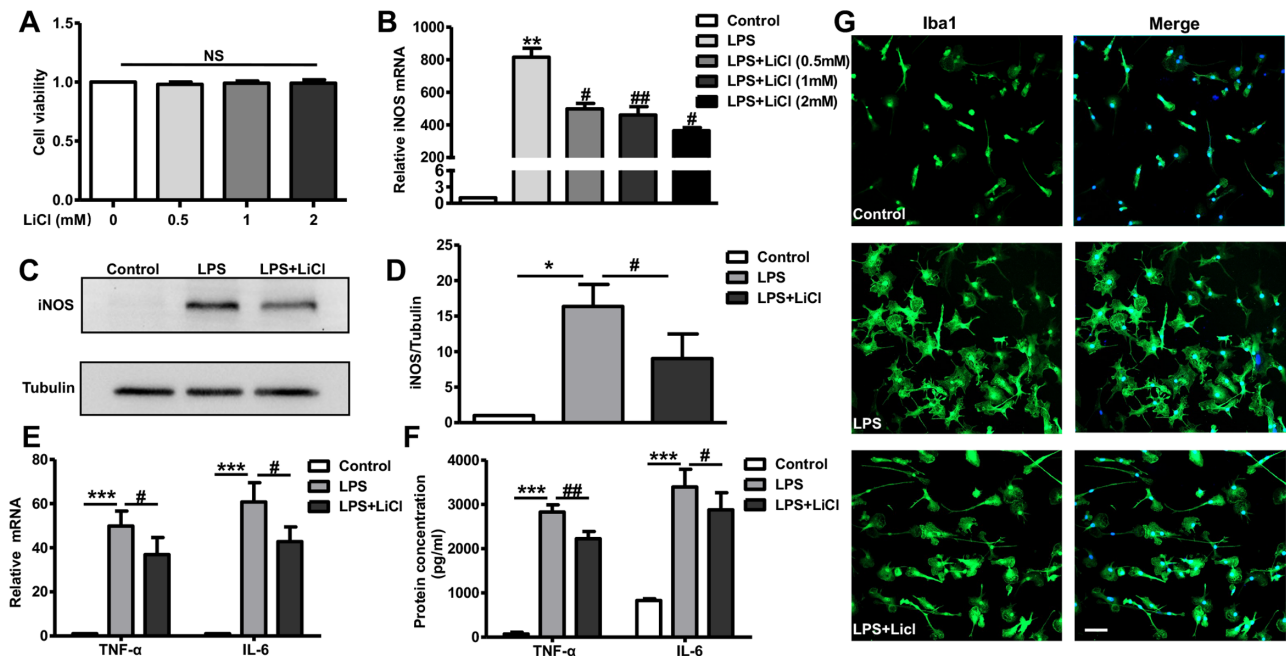
FIGURE 1. LiCl inhibited inflammatory factor production and retinal microglial activation in vitro. (**A**) The cell viability of primary retinal microglia was measured by CCK-8 assay after treatment with LiCl (0, 0.5, 1, and 2 mM) for 24 hours. (**B**) The primary retinal microglia were pretreated with LiCl (0.5, 1, and 2 mM) for 30 minutes followed by LPS (20 ng/mL) for 12 hours. The iNOS mRNA expression was detected by RT-PCR. (**C**, **D**) The primary retinal microglia were pretreated with LiCl (1 mM) for 30 minutes followed by LPS (20 ng/mL) for 24 hours. Representative protein bands of iNOS and their relative intensities are shown as a histogram. (**E**, **F**) The primary retinal microglia were pretreated with LiCl (1 mM) for 30 minutes followed by LPS (20 ng/mL) for 12 hours. The mRNA levels and protein concentrations of TNF-α and IL-6 were determined by RT-PCR and ELISA assays, respectively. (**G**) Confocal microscope images of primary retinal microglia stained with IBA1 (*green*) or DAPI (*blue*) and merged images. *Scale bar:* 50 µm. All results are presented as the mean $\pm$ SD ($n = 3$). NS, no significant difference compared with the control. Asterisks indicate significant differences from control: $^*P < 0.05$, $^{**}P < 0.01$, $^{***}P < 0.001$. Pound signs indicate significant differences from the LPS group: $^\#P < 0.05$, $^{\#\#}P < 0.01$.

shape, but LiCl inhibited these morphological changes. In conclusion, LiCl efficiently inhibited retinal microglial activation and blocked inflammation in vitro.

LiCl Suppressed LPS-Induced Retinal Microglial Activation via the PI3K/Akt/NF-κB Pathway

Recently, NF-κB signaling has been considered a master regulator of inflammation by modulating the transcription of proinflammatory factors.[17,18] In our study, LPS stimulation upregulated the phosphorylation of NF-κB and inhibitor of nuclear factor kappa B α (IκBα); in contrast, LiCl significantly reversed this effect (Figs. 2A, 2B). The immunostaining results showed that NF-κB in the control group was expressed mainly in the cytoplasm and translocated to the nucleus following LPS stimulation. However, pretreatment with lithium blocked LPS-induced nuclear translocation (Figs. 2C, 2D). In addition, BAY 11-7082, an NF-κB inhibitor, significantly blocked LPS-induced IL-6 and TNF-α expression upregulation (Fig. 2E). The PI3K/Akt pathway plays an important role in the inflammatory response and has been reported to be one of the major upstream pathways of NF-κB activation in microglia.[19–21] Herein, we found that LiCl significantly decreased the LPS-induced phosphorylation of PI3K and Akt (Figs. 2F, 2G). Taken together, these data suggest that LiCl suppresses LPS-induced retinal microglial activation via the PI3K/Akt/NF-κB pathway.

LiCl Alleviated Microglia-Mediated Neurotoxicity In Vitro

To investigate whether LiCl protects against retinal neuron damage induced by activated microglia, primary retinal neurons were cultured with microglial-derived conditioned medium (MCM) in the absence or presence of LiCl. First, primary retinal neurons were identified by microtubule-associated protein 2 (MAP2) fluorescent staining (Fig. 3A). CCK-8 data showed that culture with MCM decreased neuron viability, but LiCl could promote neuronal survival (Fig. 3B). Moreover, LiCl treatment reversed MCM-induced cell apoptosis (Figs. 3C, 3D). The accumulation of DNA breaks is an important cause of apoptosis; thus, double staining with γ-H2AX and MAP2 was performed to detect the DNA breaks in retinal neurons. As shown in Figures 3E and 3F, the number of γ-H2AX foci in MAP2-positive cells was significantly increased in the MCM-treated group compared with the control; however, LiCl treatment caused a marked decrease. Moreover, there was a clear decrease in protein expression of γ-H2AX after pretreatment with LiCl (Figs. 3G, 3H). Based on these findings, LiCl has a protective effect on retinal neurons against the neurotoxic effects triggered by microglial activation.

LiCl Relieved Retinal Inflammation in EIU Mice

Based on the in vitro results, an EIU mouse model was established to further confirm the anti-inflammatory and neuro-
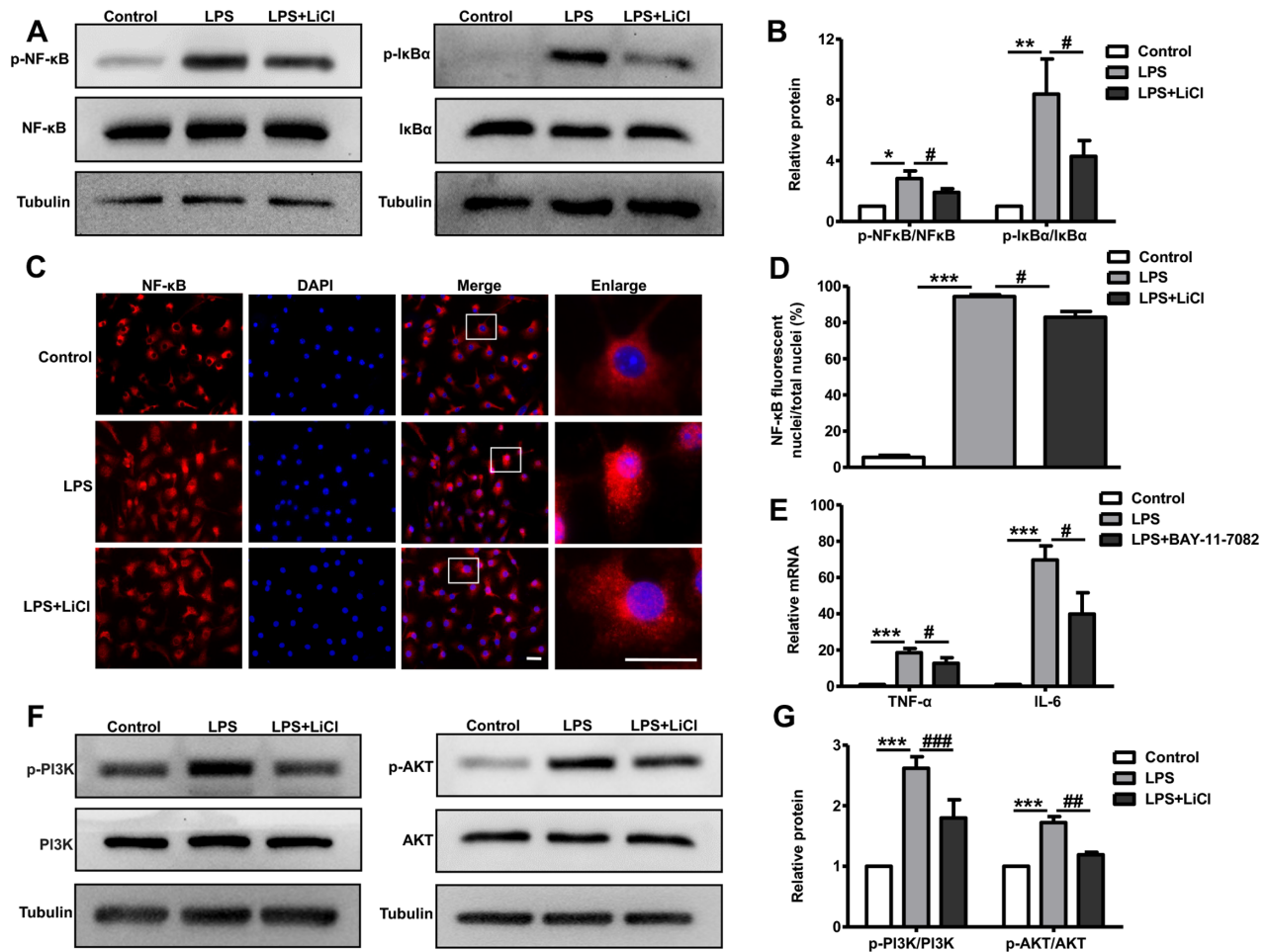
FIGURE 2. LiCl suppressed LPS-induced primary retinal microglial activation via the PI3K/Akt/NF-*κ*B pathway. The primary retinal microglia were pretreated with LiCl (1 mM) for 30 minutes followed by LPS (20 ng/mL) for 24 hours. (**A**, **B**) The protein levels of NF-*κ*B, p-NF-*κ*B, I*κ*B*α*, and p-I*κ*B*α* were detected by western blotting, and the densitometry analysis is presented as a histogram. (**C**) The nuclear translocation of the NF-*κ*B was determined using immunofluorescence assay. NF-*κ*B, *red*; DAPI, *blue*. *Scale bar*: 50 µm. (**D**) The ratio of NF-*κ*B fluorescent nuclei to the total number of nuclei is shown as a histogram. (**E**) The mRNA expression of IL-6 and TNF-*α* was measured by RT-PCR after treatment with LPS (20 ng/mL) for 12 hours in the absence or presence of the NF-*κ*B inhibitor BAY 11-7082 (1 µM). (**F**, **G**) The protein levels of PI3K, p-PI3K, Akt, and p-Akt were detected by western blotting, and the densitometry analysis is presented as a histogram. All data are presented as the mean ± SD ($n = 3$). Asterisks indicate significant differences from control: $^{*}P < 0.05$, $^{**}P < 0.01$, $^{***}P < 0.001$. Pound signs indicate significant differences from the LPS group: $^{#}P < 0.05$, $^{##}P < 0.01$, $^{###}P < 0.001$.

protective effects of LiCl in vivo. H&E staining of ocular histological sections showed that LPS induced a substantial accumulation of inflammatory cells in the vitreous that was not detected in the control group. Moreover, LiCl treatment significantly decreased the number of inflammatory cells infiltrating the vitreous cavity compared with the LPS group (Figs. 4A, 4B). Moreover, iNOS, IL-6, and TNF-*α* mRNA expression in retinas was significantly increased in the LPS group compared with the control, but LiCl injection suppressed this effect (Fig. 4C). Similarly, LiCl treatment dramatically blocked LPS-induced inflammatory factor (iNOS, IL-6, and TNF-*α*) protein level upregulation (Figs. 4D, 4E). These results suggest that LiCl dramatically alleviates LPS-induced retinal inflammation.

LiCl Suppressed LPS-Induced Retinal Microglial Activation, Proliferation, and Migration in Vivo

To confirm whether LiCl alleviates retinal inflammation by inhibition of microglial activation in vivo, fluorescent staining of whole-mount retinas and frozen sections was performed. In terms of cell morphology, IBA1 staining of retinal flatmounts showed that resting microglia appeared ramified in shape with several long branches in the control group, but the microglial presented an ameboid morphology with fewer and shorter branches in the LPS group, suggesting that LPS injection activated microglia in the retina. However, LiCl treatment inhibited morphological changes of the microglia (Figs. 5A–5C). To determine whether LiCl exposure could exert effects on the microglial proliferation, double immunofluorescence staining (IBA1 and Ki67) on retinal flatmounts was performed, and the results revealed a higher incidence of IBA1-labeled microglia colocalization of Ki67 after LPS stimulation compared with control. LiCl treatment reversed this effect, indicating that the LiCl suppressed LPS-induced microglial proliferation (Figs. 5D, 5E). In addition to the direct morphologic changes and proliferation, retinal microglia migrated to the sites of injury.[14] Our data also show that IBA1^{+} cells were present throughout the retinal layers in the control
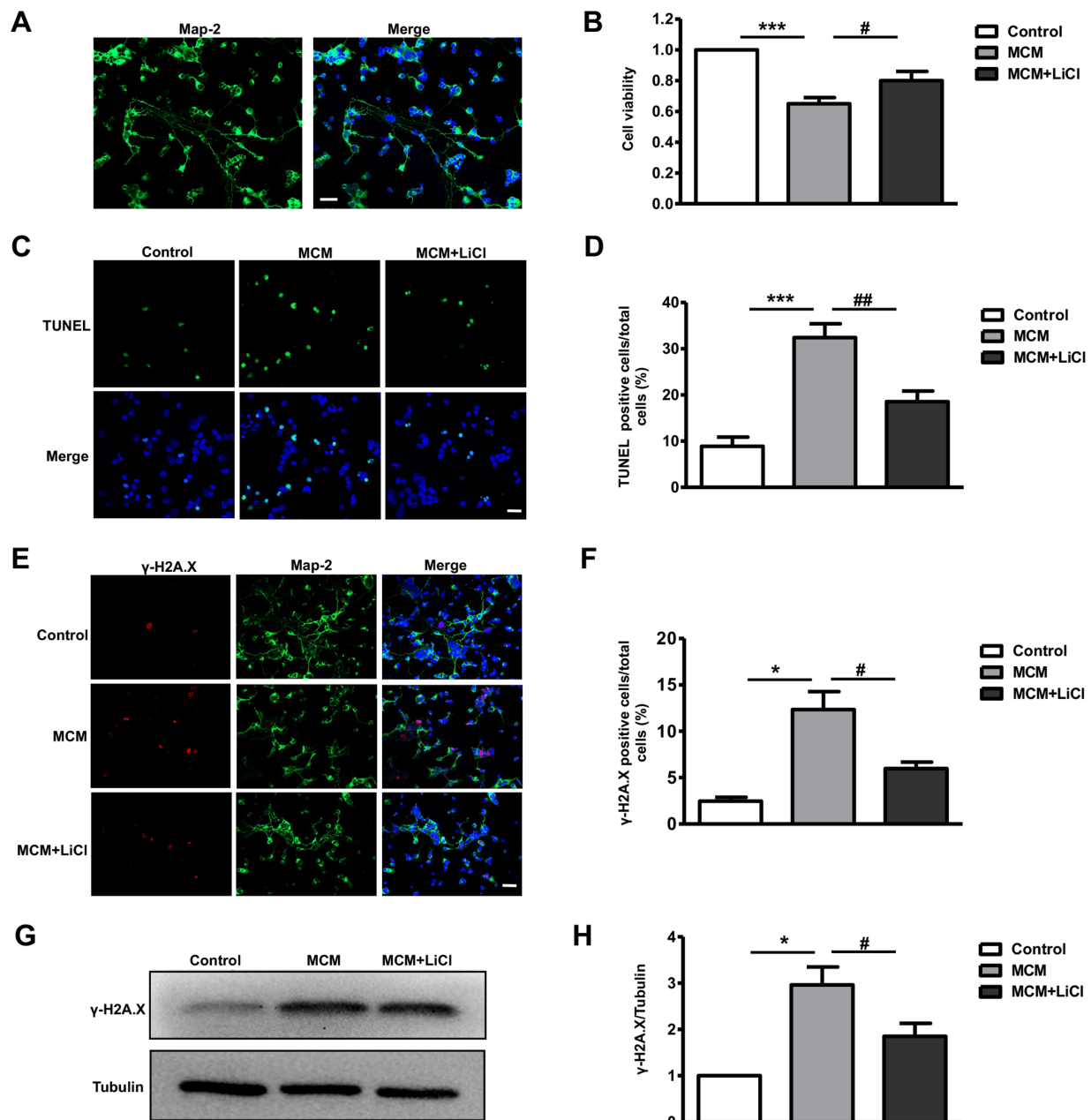
FIGURE 3. LiCl suppressed microglial activation–mediated neurotoxicity in vitro. Primary retinal neurons were cultured with conditioned medium from activated microglial in the absence or presence of lithium (1 mM). (**A**) Primary retinal neurons were identified by MAP2 (*green*) fluorescent staining. *Scale bar*: 50 µm. (**B**) Cell viability was measured by CCK-8 assay. (**C**, **D**) Fluorescence photomicrographs of TUNEL staining (*green*). The ratios of TUNEL-positive cells to the total number of cells are presented as a histogram. *Scale bar*: 50 µm. (**E**, **F**) Double-stained MAP2 (*green*) and γ-H2AX (*red*) cells used to detect DNA double-strand breaks in neurons. The ratios of γ-H2AX–positive cells to the total number of cells are presented as a histogram. *Scale bar*: 50 µm. (**G**, **H**) Protein levels of γ-H2AX were detected by western blotting, and the densitometry analysis is presented as a histogram. All results are presented as the mean $\pm$ SD ($n = 3$). Asterisks indicate significant differences from control: $^{*}P < 0.05$, $^{***}P < 0.001$. Pound signs indicate significant differences from the LPS group: $^{#}P < 0.05$, $^{##}P < 0.01$.

group, as indicated by immunostained images of the IBA1 cryosection. However, IBA1^{+} cells increased in number and migrated to the ganglion cell layer following LPS injection, and LiCl treatment significantly suppressed LPS-induced microglial migration and proliferation (Figs. 5F, 5G). These results suggest that LiCl suppressed LPS-induced retinal microglial activation, proliferation, and migration in vivo.

LiCl Exerted a Neuroprotective Effect on LPS-Induced Retinal Injury

To confirm the neuroprotective effect of LiCl in vivo, cell apoptosis was measured by TUNEL assays. As shown in Figures 6A and 6B, few apoptotic cells were observed in the retina in the control group; however, large numbers of TUNEL-positive cells were observed in the ganglion cell
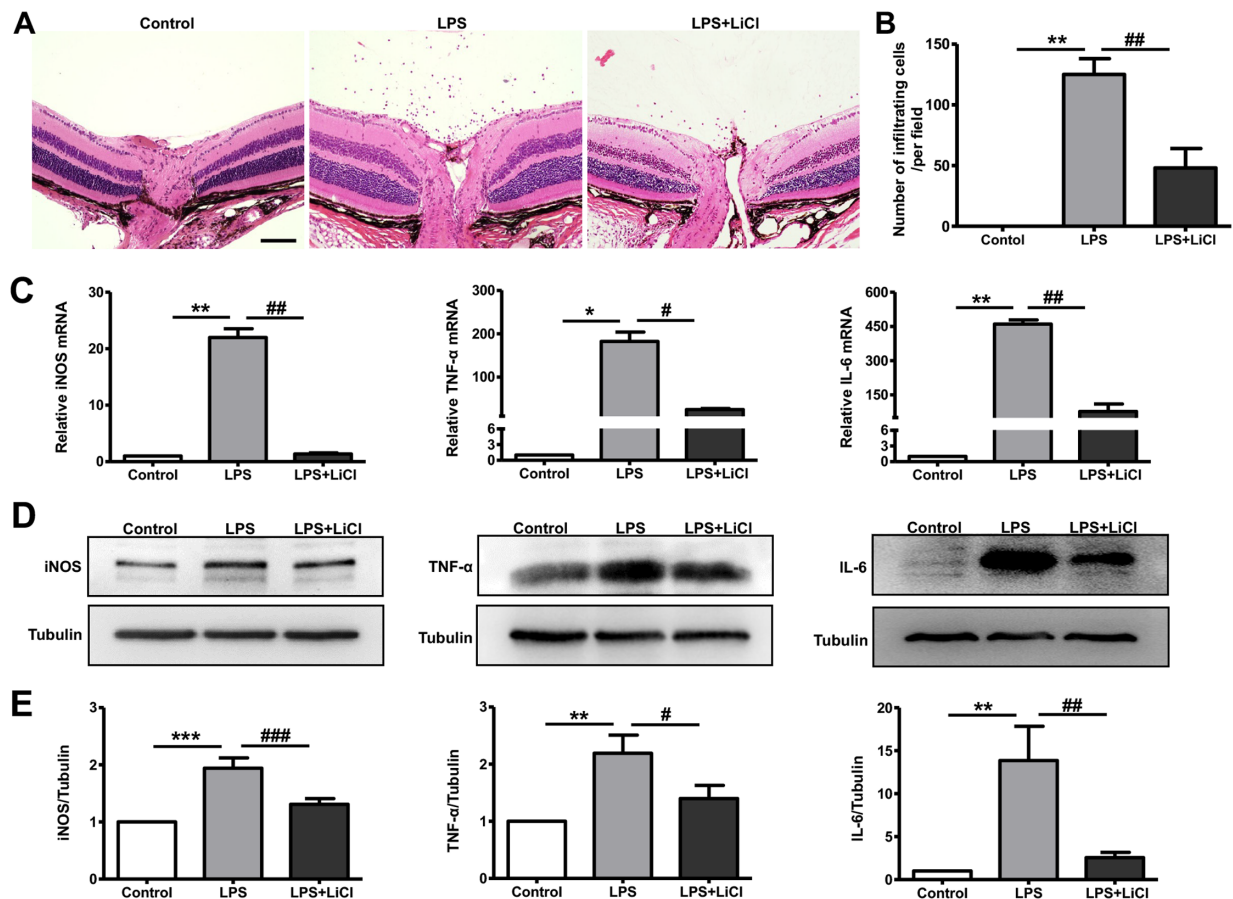
FIGURE 4. LiCl alleviated retinal inflammation in EIU mice. Mice were randomly divided into three groups: (1) control, (2) LPS, and (3) LPS + LiCl. (**A**) H&E staining images of eyeball histopathological analysis. *Scale bar*: 100 µm. (**B**) The number of inflammatory cells infiltrating the vitreous cavity around the optic disk were counted, and the results are presented as a histogram. Data are presented as the mean ± SD ($n = 5$). (**C**) Real-time PCR assays were performed to detect mRNA expression changes for iNOS, TNF-α, and IL-6 and in retinas. (**D**, **E**) iNOS, TNF-α, and IL-6 protein expression in retinas was measured by western blotting, and the densitometry analysis is presented as a histogram. Data are presented as the mean ± SD ($n = 3$). Asterisks indicate significant differences from control: $^*P < 0.05$, $^{**}P < 0.01$, $^{***}P < 0.001$. Pound signs indicate significant differences from the LPS group: $^#P < 0.05$, $^{##}P < 0.01$, $^{###}P < 0.001$.

layer after LPS injection. Interestingly, LiCl treatment significantly reduced RGCs apoptosis. Additionally, several important apoptosis-related proteins, such as caspase-3, BAX, and Bcl-2, were detected by western blot assay. As shown in Figures 6C and 6D, LPS administration increased the expression of cleaved caspase 3 and decreased the Bcl-2/BAX ratio, whereas LiCl dramatically inhibited this effect. Subsequently, spectral-domain OCT was performed to examine retinal structure. As shown in Figures 7A and 7B, LPS resulted in markedly increased retinal thickness compared with the control group, suggesting that LPS-induced inflammation caused retina edema. LiCl treatment decreased retinal thickness. In order to evaluate the function of the retina, we performed ERG in the mice. Lower ERG a-wave and b-wave amplitudes showed that LPS induced retinal functional impairment. As expected, LiCl treatment markedly improved the amplitudes of the a-waves and b-waves compared with the LPS group (Figs. 7C, 7D). These results are consistent with our in vitro data, further confirming that LiCl has an excellent neuroprotective effect on LPS-induced retinal injury.

DISCUSSION

Inhibition of microglial overactivation has been identified as a novel therapeutic strategy to manage retinal inflamma-

tory diseases. In the present study, our results demonstrated that LiCl, a common drug used to treat BD, alleviated LPS-induced retinal inflammation by inhibiting microglial activation both in vitro and in vivo. Moreover, the PI3K/Akt/NF-κB pathway may be partly involved in the molecular mechanism by which LiCl suppresses microglial activation suppression. Meanwhile, we also found that LiCl treatment could markedly suppress microglial-mediated neurotoxicity and protect the retinal function from inflammatory insult.

Microglia are the essential resident immune cells in the retina and are most important for maintaining retinal homeostasis and the response to neuroinflammation. Under different conditions, activated microglia may acquire two different kinds of polarization: proinflammatory classically activated M1 microglia and anti-inflammatory selectively activated M2 microglia.[22] It has been reported that LiCl alleviates titanium nanoparticle–mediated inflammatory reactions and enhances the osteogenic differentiation of rat bone marrow mesenchymal stem cells by driving M1 macrophages to the M2 phenotype.[23] In the present study, our results indicate that LiCl treatment suppresses LPS-induced upregulation of iNOS, IL-6, and TNF-α, which are the markers of M1 microglia. However, no expression changes in the markers of M2 microglia, such as Arg-1 and IL-4, were observed (data not shown), suggesting that the effect of
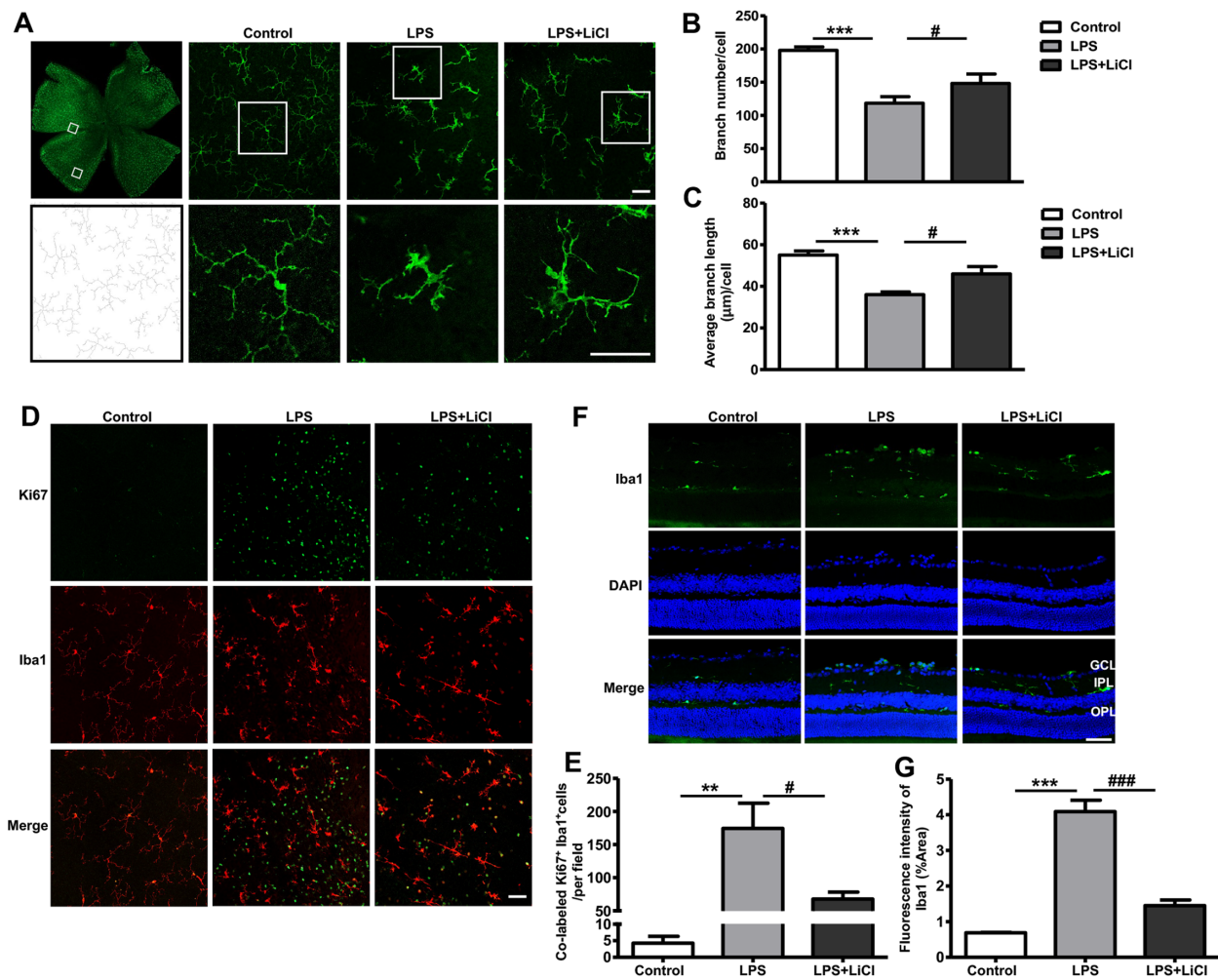
FIGURE 5. LiCl suppressed retinal microglial activation, proliferation, and migration in vivo. (**A**) Representative confocal images of retinal flatmounts stained with IBA1 (*green*). *Scale bar*: 50 µm. (**B**, **C**) The branch numbers and average branch lengths of microglia were calculated and are presented as a histogram. Data are presented as the mean ± SD (*n* = 4). (**D**) Representative confocal images of retinal flatmounts co-stained with Ki67 (*green*) and IBA1 (*red*). *Scale bar*: 50 µm. (**E**) The co-labeled Ki67- and IBA1-positive cells were counted and are presented as a histogram. (**F**) Fluorescence photomicrographs of retinal cryosection stained with IBA1 (*green*) and DAPI (*blue*). *Scale bar*: 50 µm. (**G**) Quantification of the fluorescence intensity of IBA1 (% area) is shown. Data are presented as the mean ± SD (*n* = 5). GCL, ganglion cell layer; IPL, inner plexiform layer; OPL, outer plexiform layer. Asterisks indicate significant differences from control: $^{***}P < 0.001$. Pound signs indicate significant differences from the LPS group: $^{###}P < 0.001$.

LiCl focus on inhibiting M1 microglia in control retinal inflammation.

Interestingly, the effect of LiCl on inflammatory cytokine production was much more pronounced in vivo than in vitro in our study. There may be several reasons for this result. For example, a recent study suggested that activated microglia is associated with retinal capillary constriction and slowed blood flow.[24] LiCl treatment inhibits microglia activation, which may protect retinal blood circulation indirectly and help with the clearance of inflammatory factors. Moreover, the retinal immune environment is very complex. Immune cells in the retinal blood vessels and even retinal astrocytes may contribute to LiCl inflammation suppression. Furthermore, the mRNA and protein were extracted from pure microglia in the in vitro experiments, whereas they were obtained from whole mice retina in the in vivo experiments. The reasons mentioned above may lead to inconsistencies between in vitro and in vivo experimental paradigms.

Moreover, our results suggest that the PI3K/Akt/NF-κB pathway may be partly involved in the molecular mechanism by which LiCl mediates microglial activation suppression. NF-κB plays a central role in inflammatory diseases; classic NF-κB is composed of the p65 and p50 subunits and normally binds to its inhibitor IκBα in the cytoplasm as an inactive dimer in the resting state. Upon receiving an activating signal, IκBα is phosphorylated by the IκB kinase complex, and then NF-κB dimers are released and move into the nucleus to bind to specific sites in the DNA, regulating the transcription of proinflammatory factors, such as iNOS, IL-6, and TNF-α.[23] In the present study, we demonstrated that LiCl suppressed LPS-induced NF-κB and IκBα phosphorylation and NF-κB nuclear translocation, findings that are consistent with a previous study by Mitchell and Carmody.[17] That study indicated that LPS-induced NF-κB activation is directly regulated by phosphorylation of PI3K/Akt in microglial cells, consequently implying that PI3K/Akt may be useful to prevent neuroinflammation. Therefore,
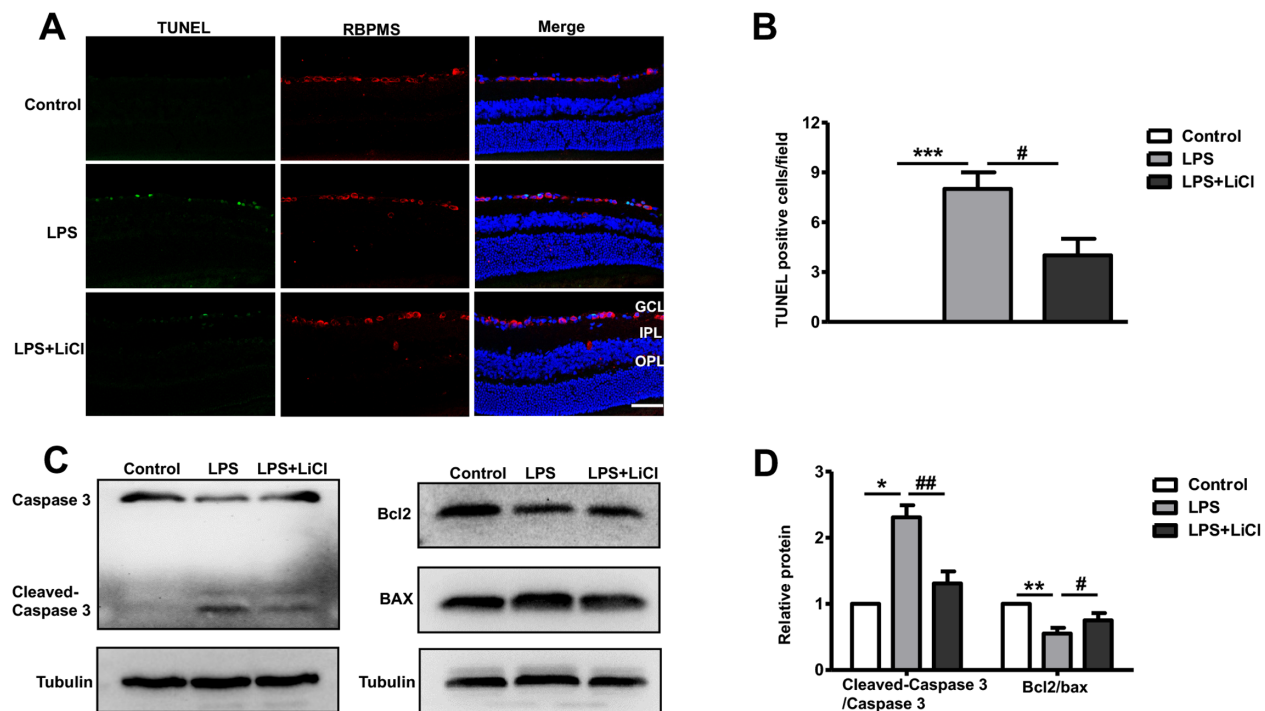
FIGURE 6. LiCl prevented RGC apoptosis in EIU mice. (**A**) Confocal images of retinal cryosection stained with TUNEL (*green*), RBPMS (*red*), and DAPI (*blue*). *Scale bar*: 50 µm. (**B**) TUNEL-positive cells were counted and are presented as a histogram. Data are presented as the mean ± SD ($n = 3$). (**C**) Representative gel images of apoptosis-related proteins (caspase 3, cleaved caspase 3, Bcl-2, and BAX). (**D**) Densitometry quantification of the cleaved caspase 3 and the ratio of Bcl-2 to BAX. The data represent the mean ± SD ($n = 3$). Asterisks indicate significant differences from control: $^*P < 0.05$, $^{**}P < 0.01$, $^{***}P < 0.001$. Pound signs indicate significant differences from the LPS group: $^\#P < 0.05$, $^{\#\#}P < 0.01$.

modulation of the PI3K/Akt/NF-κB pathway is also considered to be a good approach for the treatment of many neuropathological diseases by inhibiting proinflammatory gene expression.[25–27] In the present study, we demonstrated that LiCl suppressed LPS-induced NF-κB, IκBα, Akt, and PI3K phosphorylation and NF-κB nuclear translocation. Therefore, LiCl alleviated LPS-induced retinal inflammation, perhaps partly by inhibiting M1 microglial activation via the PI3K/Akt/NF-κB pathway.

In addition to its strong anti-inflammatory effect, LiCl also has a powerful neuroprotective effect in vision system injury. In an optic nerve injury model in rats, the neuroprotective effects of LiCl can be attributed to various mechanisms, such as upregulation of antiapoptotic proteins, suppression of proinflammatory molecules and proapoptotic factors, and decreased nitric oxide.[28] Several mediators, including *N*-methyl-D-aspartate receptors, the PI3K/Akt pathway, cytoprotective Bcl-2, and glycogen synthase kinase-3 beta (GSK-3β), are implicated in the process underlying LiCl-induced neuroprotection, which could promote RGC survival and axon regeneration.[29–31] In the present study, our results also indicated that LiCl dramatically decreased the expression of cleaved caspase 3 and increased the Bcl-2/BAX ratio, thus inhibiting microglial-induced apoptosis of the retinal neurocytes. Moreover, our previous study also showed that, to offer neuroprotection in the face of ischemia-induced damage, LiCl might promote DNA nonhomologous end-joining repair by upregulating ligase IV.[13] In addition, another previous study suggested that LiCl enhanced neuronal survival in ischemic–reperfusion retinal injury by GSK-3β inhibition.[32] Taken together, the

neuroprotective function of LiCl was reflected in two ways in our study. On the one hand, LiCl could inhibit microglial activation, subsequently reducing the secretion of inflammatory cytokines that damage retinal neurons. On the other hand, LiCl treatment could promote the survival of already damaged neurons, reducing DNA breaks and cell apoptosis. However, the underlying molecular mechanism by which LiCl promotes retinal neuron survival in microglial-mediated damage requires further investigation.

In the present study, we detected RGC apoptosis only after LPS stimulation, which might be due to the EIU mice being induced by intravitreal injection of LPS, and RGCs located in the innermost of retina were first to suffer damage. In addition, our OCT data showed that LPS-induced inflammation caused total retinal edema. Thus, although other retinal cells, such as photoreceptors, did not undergo apoptosis, their function might be impaired by inflammation. LiCl treatment contributed to reduced RGC apoptosis and alleviated retinal edema, both reasons for the ERG changes that we observed.

In summary, microglia play an important role in neuroinflammatory conditions; however, microglial overactivation is definitely harmful in the pathophysiological process in numerous retinal diseases. Therefore, an ideal treatment strategy should offer both anti-inflammatory and neuroprotective effects; interestingly, LiCl exhibited these powerful dual effects in the present study. This study not only provides new insights into the mechanism of retinal neuroprotection but also extends the application of LiCl to the treatment of retinal inflammatory disorders.
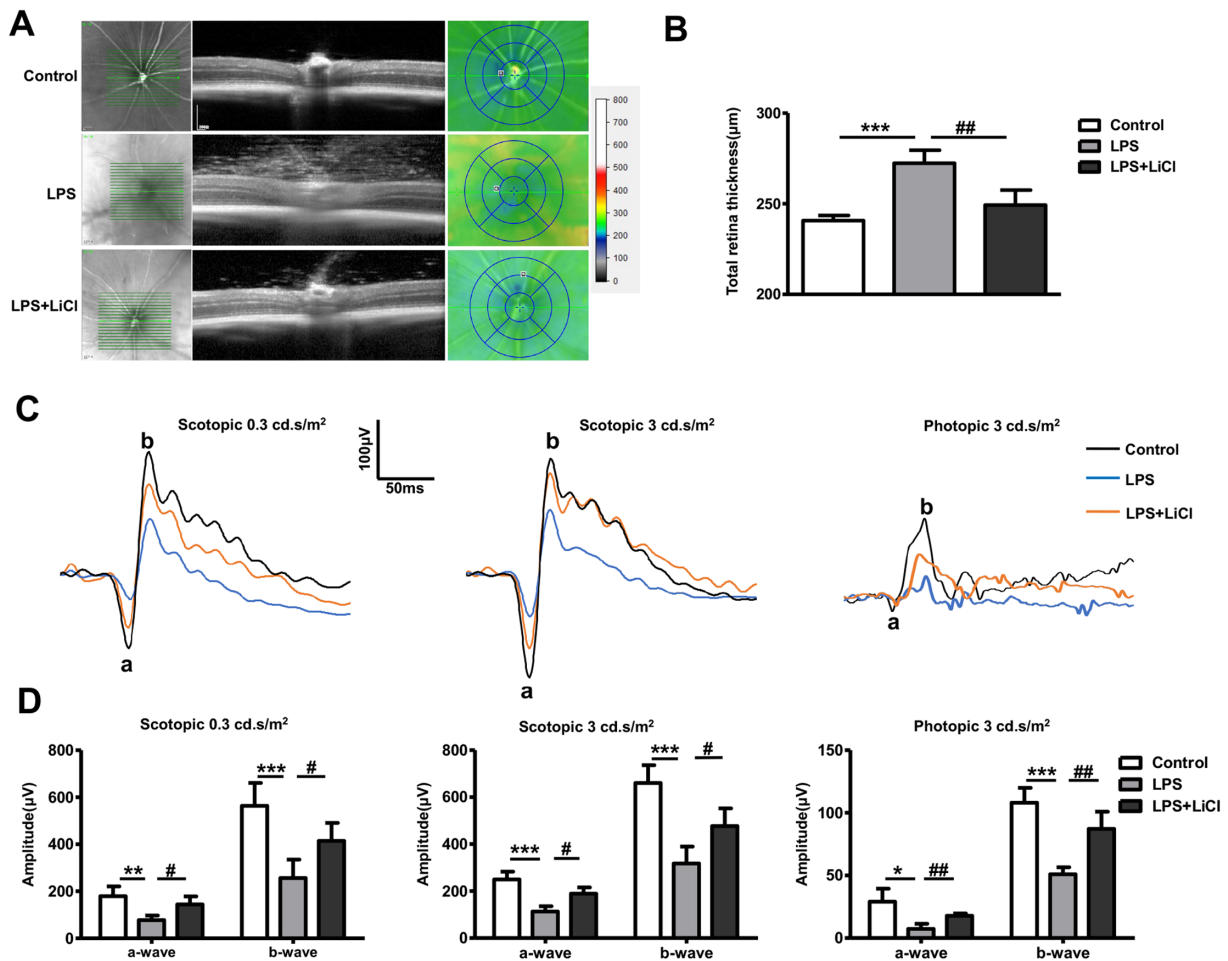
Investigative Ophthalmology & Visual Science

FIGURE 7. LiCl pretreatment relieved the retinal edema and function impairment induced by LPS in the EIU mice model. (**A**, **B**) Retinal structures were evaluated by spectral-domain OCT. Total retinal thicknesses were calculated and are presented as a histogram. (**C**) Retinal function was evaluated by ERG examination under scotopic (0.3 cd·s/m^2 and 3 cd·s/m^2) and photopic (3 cd·s/m^2) light intensity. (**D**) The a-wave and b-wave amplitudes are presented as a histogram. The data are presented as the mean ± SD ($n = 5$). Asterisks indicate significant differences from control: $^{**}P < 0.01$, $^{***}P < 0.001$. Pound signs indicate significant differences from the LPS group: $^{#}P < 0.05$, $^{##}P < 0.01$.

References

1. Perez VL, Caspi RR. Immune mechanisms in inflammatory and degenerative eye disease. *Trends Immunol*. 2015;36:354–363.
2. Muzio L, Viotti A, Martino G. Microglia in neuroinflammation and neurodegeneration: From understanding to therapy. *Front Neurosci*. 2021;15:742065.
3. Rashid K, Akhtar-Schaefer I, Langmann T. Microglia in retinal degeneration. *Front Immunol*. 2019;10:1975.
4. Streit WJ, Mrak RE, Griffin WS. Microglia and neuroinflammation: A pathological perspective. *J Neuroinflammation*. 2004;1:14.
5. Huang Z, Zhou T, Sun X, et al. Necroptosis in microglia contributes to neuroinflammation and retinal degeneration through TLR4 activation. *Cell Death Differ*. 2018;25:180–189.
6. Skold M, Rolstad S, Joas E, et al. Regional lithium prescription rates and recurrence in bipolar disorder. *Int J Bipolar Disord*. 2021;9:18.
7. Nassar A, Azab AN. Effects of lithium on inflammation. *ACS Chem Neurosci*. 2014;5:451–458.
8. Dong H, Zhang X, Dai X, et al. Lithium ameliorates lipopolysaccharide-induced microglial activation via inhibition of toll-like receptor 4 expression by activating the PI3K/Akt/FoxO1 pathway. *J Neuroinflammation*. 2014;11:140.
9. Habib MZ, Ebeid MA, El Faramawy Y, et al. Effects of lithium on cytokine neuro-inflammatory mediators, Wnt/β-catenin signaling and microglial activation in the hippocampus of chronic mild stress-exposed rats. *Toxicol Appl Pharmacol*. 2020;399:115073.
10. Fan M, Song C, Wang T, et al. Protective effects of lithium chloride treatment on repeated cerebral ischemia–reperfusion injury in mice. *Neurol Sci*. 2015;36:315–321.
11. Ciftci E, Karacay R, Caglayan A, et al. Neuroprotective effect of lithium in cold- induced traumatic brain injury in mice. *Behav Brain Res*. 2020;392:112719.

12. Forlenza OV, De-Paula VJ, Diniz BS. Neuroprotective effects of lithium: Implications for the treatment of Alzheimer's disease and related neurodegenerative disorders. *ACS Chem Neurosci*. 2014;5:443–450.

13. Yang Y, Wu N, Tian S, et al. Lithium promotes DNA stability and survival of ischemic retinal neurocytes by upregulating DNA ligase IV. *Cell Death Dis*. 2016;7:e2473.

14. Han X, Chen X, Chen S, et al. Tetramethylpyrazine attenuates endotoxin-induced retinal inflammation by inhibiting microglial activation via the TLR4/NF-κB signalling pathway. *Biomed Pharmacother*. 2020;128:110273.

15. Cheng Z, Yang Y, Duan F, et al. Inhibition of Notch1 signaling alleviates endotoxin-induced inflammation through modulating retinal microglia polarization. *Front Immunol*. 2019;10:389.

16. Wang F, Jiang Z, Lou B, et al. αB-Crystallin alleviates endotoxin-induced retinal inflammation and inhibits microglial activation and autophagy. *Front Immunol*. 2021;12:641999.

17. Mitchell JP, Carmody RJ. NF-κB and the transcriptional control of inflammation. *Int Rev Cell Mol Biol*. 2018;335:41–84.

18. Baldwin AS, Jr. Series introduction: The transcription factor NF-κB and human disease. *J Clin Invest*. 2001;107:3–6.

19. Lou Y, Wang C, Tang Q, et al. Paeonol inhibits IL-1β-induced inflammation via PI3K/Akt/NF-κB pathways: In vivo and vitro studies. *Inflammation*. 2017;40:1698–1706.

20. Jayasooriya RG, Lee KT, Kang CH, et al. Isobutyrylshikonin inhibits lipopolysaccharide-induced nitric oxide and prostaglandin E2 production in BV2 microglial cells by suppressing the PI3K/Akt-mediated nuclear transcription factor-κB pathway. *Nutr Res*. 2014;34:1111–1119.

21. Han MH, Lee WS, Nagappan A, et al. Flavonoids isolated from flowers of *Lonicera japonica* Thunb. inhibit inflammatory responses in BV2 microglial cells by suppressing TNF-α and IL-β through PI3K/Akt/NF-κB signaling pathways. *Phytother Res*. 2016;30:1824–1832.

22. Ji J, Xue TF, Guo XD, et al. Antagonizing peroxisome proliferator-activated receptor γ facilitates M1-to-M2 shift of microglia by enhancing autophagy via the LKB1–AMPK signaling pathway. *Aging Cell*. 2018;17:e12774.

23. Yang C, Wang W, Zhu K, et al. Lithium chloride with immunomodulatory function for regulating titanium nanoparticle-stimulated inflammatory response and accelerating osteogenesis through suppression of MAPK signaling pathway. *Int J Nanomedicine*. 2019;14:7475–7488.

24. Mills SA, Jobling AI, Dixon MA, et al. Fractalkine-induced microglial vasoregulation occurs within the retina and is altered early in diabetic retinopathy. *Proc Natl Acad Sci USA*. 2021;118:e2112561118.

25. Dong L, Li YZ, An HT, et al. The E3 ubiquitin ligase c-Cbl inhibits microglia-mediated CNS inflammation by regulating PI3K/Akt/NF-κB pathway. *CNS Neurosci Ther*. 2016;22:661–669.

26. Xu X, Xu H, Ren F, Huang L, Xu J, Li F. Protective effect of scorpion venom heat-resistant synthetic peptide against PM2.5-induced microglial polarization via TLR4-mediated autophagy activating PI3K/AKT/NF-κB signaling pathway. *J Neuroimmunol*. 2021;355:577567.

27. Dilshara MG, Lee KT, Choi YH, et al. Potential chemoprevention of LPS-stimulated nitric oxide and prostaglandin E(2) production by α-L-rhamnopyranosyl-(1→6)-β-D-glucopyranosyl-3-indolecarbonate in BV2 microglial cells through suppression of the ROS/PI3K/Akt/NF-κB pathway. *Neurochem Int*. 2014;67:39–45.

28. Ala M, Mohammad Jafari R, Nematian H, et al. Neuroprotective effect of intravitreal single-dose lithium chloride after optic nerve injury in rats. *Curr Eye Res*. 2021;46:558–567.

29. Li X, Bijur GN, Jope RS. Glycogen synthase kinase-3β, mood stabilizers, and neuroprotection. *Bipolar Disord*. 2002;4:137–144.

30. Huang X, Wu DY, Chen G, Manji H, Chen DF. Support of retinal ganglion cell survival and axon regeneration by lithium through a Bcl-2-dependent mechanism. *Invest Ophthalmol Vis Sci*. 2003;44:347–354.

31. Schuettauf F, Rejdak R, Thaler S, et al. Citicoline and lithium rescue retinal ganglion cells following partial optic nerve crush in the rat. *Exp Eye Res*. 2006;83:1128–1134.

32. Zhang J, Lai ZP, Chen P, Ying Y, Zhuang J, Yu KM. Glycogen synthase kinase-3β inhibitor SB216763 promotes DNA repair in ischemic retinal neurons. *Neural Regen Res*. 2021;16:394–400.